

Cite this: *Chem. Sci.*, 2015, 6, 1282Received 9th October 2014  
Accepted 5th November 2014DOI: 10.1039/c4sc03095h  
[www.rsc.org/chemicalscience](http://www.rsc.org/chemicalscience)

## Introduction

Phosphonate natural products are a class of compounds featuring a C–P bond.<sup>1</sup> Many of these natural products show interesting and potent bioactivity. For instance, fosfomycin is an antibiotic in clinical use, while phosphonothricin tripeptide (PTT) is a widely used herbicide (Fig. 1).<sup>1</sup> The bioactivities of

phosphonates are generally attributed to their C–P bonds, which mimic, but are much more stable than, the corresponding O–P bond of phosphate esters.<sup>1</sup> In recent years phosphonate natural products have drawn attention not only because of their bioactivity, but also because of the plethora of unusual and interesting chemistries associated with the biosynthesis of these molecules.<sup>2,3</sup>

Originally isolated from *Streptomyces lavendofoliae* 630, fosfazinomycins (Fig. 1) are natural phosphonates with antifungal activity.<sup>4,5</sup> Compared to fosfazinomycin B (fosB), fosfazinomycin A (fosA) contains an extra Val residue at the N-terminus. The most interesting structural feature of fosfazinomycins is the unusual hydrazide linkage between the carboxylic acid of Arg and the phosphonic acid. Although the structures of these antibiotics were elucidated three decades ago, information on their biosynthesis was unavailable until our very recent description of the biosynthetic gene cluster.<sup>6</sup>

Very little is known about how nitrogen–nitrogen bonds are fashioned in nature. In principle, three different pathways can

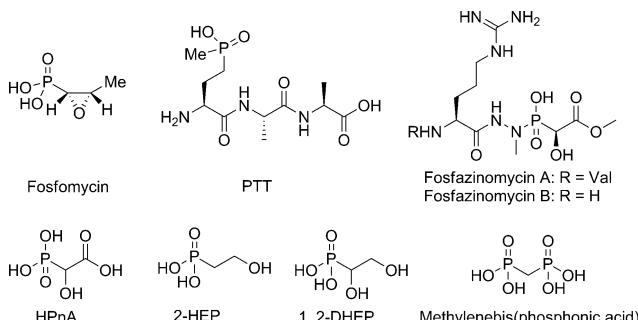


Fig. 1 Structures of select phosphonates.

<sup>a</sup>Institute for Genomic Biology, University of Illinois at Urbana-Champaign, Urbana, IL 61801, USA<sup>b</sup>Department of Chemistry, University of Illinois at Urbana-Champaign, Urbana, IL 61801, USA. E-mail: vdonk@illinois.edu<sup>c</sup>Howard Hughes Medical Institute, USA

† Electronic supplementary information (ESI) available: Supplementary figures, molecular biology procedures, enzyme purifications, and synthetic procedures for the preparation of substrates and standards and their spectroscopic characterization. See DOI: 10.1039/c4sc03095h

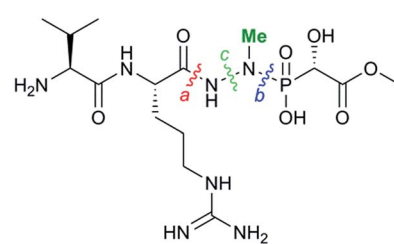


Fig. 2 Three disconnections to generate the central hydrazide core of fosfazinomycins.

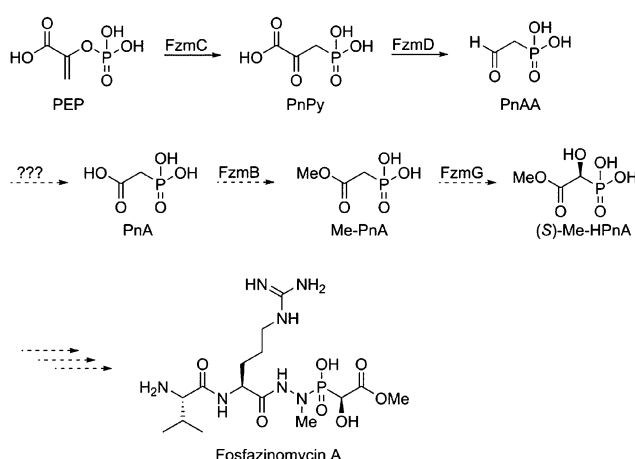


be envisioned in the case of fosfazinomycin (Fig. 2). The hydrazide moiety could be initially attached to the phosphonate and then coupled to the Arg or the Val–Arg dipeptide (retrosynthetic disconnection *a*, Fig. 2). Alternatively, the hydrazide could be formed on the Arg or the Val–Arg dipeptide and then be condensed with the phosphonic acid (disconnection *b*), or the hydrazide could be formed from an amide and phosphonamide (disconnection *c*). Herein we report the first *in vitro* biochemical investigation of fosfazinomycin biosynthesis. Our studies assign the function of the enzymes involved in the formation of (*S*)-methyl 2-hydroxy-2-phosphono-acetate ((*S*)-Me-HPnA) from phosphonoacetaldehyde (PnAA, Scheme 1). FzmB is shown to be an *O*-methyltransferase that methylates phosphonoacetate, and the  $\alpha$ -ketoglutarate ( $\alpha$ -KG) dependent non-heme iron dioxygenase FzmG is demonstrated to catalyse the oxidation of two different substrates. Moreover, evaluation of various different potential substrates of the *N*-methyltransferase FzmH strongly suggests that fosfazinomycins are biosynthesized through a convergent pathway that is consistent with disconnection *b* (Fig. 2).

## Results

The *fzmB* and *fzmG* genes were amplified by the polymerase chain reaction (PCR) from the fosmids MMG 358 and 360,<sup>7</sup> respectively, that both harbour the fosfazinomycin gene cluster. The amplified genes were inserted into the expression vector pET-15b. Both proteins were expressed in *Escherichia coli* as N-terminal hexahistidine-tagged constructs and purified by immobilized metal affinity chromatography (IMAC) to near homogeneity (>90% purity) according to SDS/PAGE analysis (Fig. S1 in the ESI<sup>†</sup>).

With the soluble proteins in hand, we first tested the activity of His<sub>6</sub>–FzmB with two putative substrates, phosphonoacetate (PnA) and *rac*-2-hydroxy-2-phosphono-acetate (*rac*-HPnA) (Fig. 1). When PnA was used as substrate in the presence of *S*-adenosyl methionine (SAM), *ca.* 90% conversion to the methyl ester was achieved according to analysis by <sup>31</sup>P NMR



Scheme 1 Previously proposed initial steps of the biosynthetic pathway of fosfazinomycin A.

spectroscopy. The product was confirmed to be Me-PnA by spiking with an authentic synthetic standard (Fig. S2<sup>†</sup>). In the absence of either the enzyme or SAM, only the starting material was recovered. In addition, complete conversion of *rac*-HPnA to Me-HPnA was observed in the presence of His<sub>6</sub>–FzmB and SAM (Fig. S3<sup>†</sup>). Therefore His<sub>6</sub>–FzmB was able to methylate both enantiomers of HPnA. The high conversions in both reactions made it difficult to conclude whether PnA or HPnA would be the physiological substrate of FzmB. To further study its substrate tolerance, methylenebis(phosphonic acid) (Fig. 1) and malonic acid were tested as close analogs of PnA, but product was not detected in either reaction.

Next we investigated the function of the putative  $\alpha$ -KG dependent dioxygenase FzmG. Initially Me-PnA was tested, resulting in complete conversion of Me-PnA to Me-HPnA (Fig. 3A and B). The reaction was enzyme-catalysed and  $\alpha$ -KG was essential for catalysis (Fig. 3C and E). In addition, the common reductant L-ascorbate accelerated the reaction (Fig. 3A and D). Recently Hammerschmidt and co-workers have determined the absolute configuration of Me-HPnA in fosfazinomycins to be *S* by comparison of chemically synthesized standards to the fragments generated from acid-mediated hydrolysis of fosfazinomycins.<sup>8</sup> In addition, they found that Me-HPnA was configurationally stable in water at slightly acidic pH but completely racemized at pH 7–8. Given its ease to racemize at the pH we used for the enzymatic assays, we did not attempt to determine the stereochemistry of our enzymatic product. PnA was also incubated with His<sub>6</sub>–FzmG. Under the same conditions that resulted in complete consumption of Me-PnA, the conversion of PnA was only 30%; the product was confirmed to be HPnA by spiking with authentic synthetic standard (Fig. S4<sup>†</sup>).

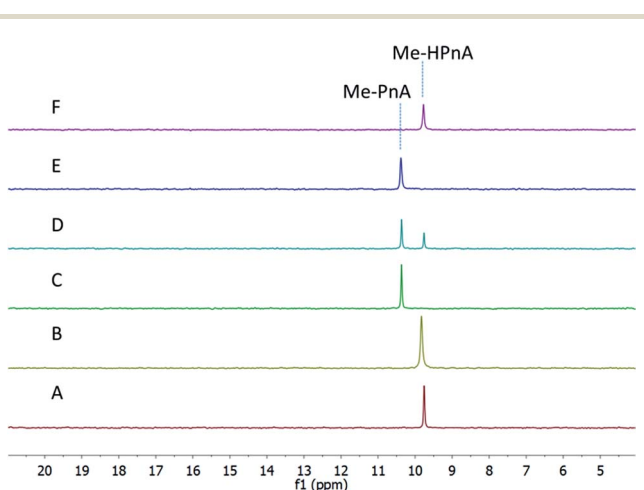


Fig. 3 <sup>31</sup>P NMR spectra of the products obtained by incubation of His<sub>6</sub>–FzmG with Me-PnA. (A) NMR spectrum of the reaction mixture containing Me-PnA, O<sub>2</sub>,  $\alpha$ -KG, Fe(II), L-ascorbate, and His<sub>6</sub>–FzmG. (B) NMR spectrum of the enzymatic reaction mixture spiked with authentic standard of Me-HPnA. (C) NMR spectrum of the reaction mixture in the absence of  $\alpha$ -KG. (D) NMR spectrum of the reaction mixture in the absence of L-ascorbate. (E) NMR spectrum of the reaction mixture in the absence of His<sub>6</sub>–FzmG. (F) NMR spectrum of authentic Me-HPnA.

DhpA is another  $\alpha$ -KG dependent non-heme iron dioxygenase that hydroxylates 2-hydroxyethyl-phosphonate (2-HEP) to generate 1,2-dihydroxyethylphosphonate (1,2-DHEP) (Fig. 1) during the biosynthesis of dehydrophos.<sup>9,10</sup> FzmG and DhpA share 45% and 55% sequence identity and similarity, respectively.<sup>6</sup> The high sequence identity prompted us to investigate whether these two enzymes could act on each other's substrates. His<sub>6</sub>-FzmG completely converted 2-HEP to 1,2-DHEP (Fig. S5†), whereas His<sub>6</sub>-DhpA did not accept Me-PnA as a substrate (Fig. S6†). 2-Aminoethylphosphonate (2-AEP) was also incubated with His<sub>6</sub>-FzmG, but no activity was observed.

To examine the possibility that hydroxylation at the alpha carbon of the phosphonate moiety of fosfazinomycins occurs before the oxidation at the beta carbon, phosphonoacetaldehyde (PnAA) was incubated with His<sub>6</sub>-FzmG. In this model, 2-hydroxy-2-phosphono-acetaldehyde (HPnAA) was expected to be the product. Upon incubation, the PnAA peak (9 ppm) in the <sup>31</sup>P NMR spectrum indeed disappeared and a new peak appeared at 13.7 ppm (Fig. 4A and B). A <sup>1</sup>H-<sup>31</sup>P HMBC NMR spectrum suggested the newly formed product might be PnA rather than the anticipated HPnAA. This assignment was confirmed by spiking with authentic PnA (Fig. 4C). This unexpected result was quite interesting, because in our proposed biosynthetic pathway (Scheme 1) a canonical aldehyde dehydrogenase was invoked to convert PnAA to PnA, but such a gene is absent in the gene cluster. The current data suggest that FzmG could catalyse two distinct steps in fosfazinomycin biosynthesis, oxidation of PnAA to PnA and hydroxylation of Me-PnA.

To further test this hypothesis, we determined the kinetic parameters of His<sub>6</sub>-FzmG towards the substrates. By

Table 1 Apparent steady-state kinetic parameters of His<sub>6</sub>-FzmG towards various substrates

	$k_{\text{cat}}$ (s <sup>-1</sup> )	$K_m$ (mM)	$k_{\text{cat}}/K_m$ (M <sup>-1</sup> s <sup>-1</sup> )
Me-PnA	0.27 ± 0.01	0.08 ± 0.02	$3 \times 10^3$
PnA	0.17 ± 0.01	8 ± 1	$2 \times 10^2$
2-HEP	0.35 ± 0.02	0.21 ± 0.04	$1.7 \times 10^3$
PnAA	0.46 ± 0.08	0.8 ± 0.3	$6 \times 10^2$

monitoring the O<sub>2</sub> consumption rate using a Hansatech O<sub>2</sub> electrode, the apparent steady-state kinetic parameters for several substrates were determined (Table 1). Clearly, MePnA is a much better substrate than PnA, suggesting that methylation occurs before hydroxylation. Furthermore, PnAA is also a reasonably good substrate (Fig. S7†), consistent with FzmG catalysing two steps in the biosynthesis of fosfazinomycin.

After the successful *in vitro* reconstitution of the biosynthesis of Me-HPnA, we next sought to decipher how this moiety might be incorporated into fosfazinomycins. At least two possible routes can be envisioned from (S)-Me-HPnA to fosfazinomycin B (Scheme 2). In route a, (S)-Me-HPnA is first transformed into the phosphonamide 1, then converted to the phosphorylhydrazide 2, which would condense with arginine to afford desmethyl fosfazinomycin B (desmethyl-fosB) in a linear pathway. Compound 2 could also be formed by condensation of Me-HPnA with a hydrazine derivative. Alternatively, arginine could be converted to the arginine hydrazide 3 (Arg-NHNH<sub>2</sub>) and joined with (S)-Me-HPnA to generate desmethyl-fosB in a convergent pathway (route b). Finally, compound 1 could be linked to arginine amide by unprecedented chemistry (not shown). To date, we have not been successful in reconstituting the activity of the enzymes that have been proposed to be involved in N-N bond formation and the condensation reactions that install the linkages to the Arg and Me-HPnA.<sup>6</sup> However, we were able to obtain important information on the timing of these processes in an indirect way. The fosfazinomycins contain a methyl group on the nitrogen directly attached to the phosphonate, and in principle, the methyl group could be introduced on one of four putative intermediates, compounds 1–3 and desmethyl-fosB (Scheme 2). Determination of the substrate of the putative methyltransferase FzmH could therefore provide key insights on the manner in which the central core of fosfazinomycin is assembled.

The gene encoding the putative N-methyltransferase FzmH was amplified by PCR from the genomic DNA of another fosfazinomycin producing strain, *Streptomyces* sp. WM6372, and ligated into the expression vector pET-15b. The corresponding protein was expressed in *E. coli* as an N-terminal hexahistidine-tagged construct and purified by IMAC (Fig. S8†). All four putative substrates for FzmH were chemically synthesized (see ESI for details†). Compounds 1, 2, or desmethyl-fosB were incubated with His<sub>6</sub>-FzmH in the presence of SAM and S-adenosyl homocysteine (AdoHcy) nucleosidase to prevent product inhibition by AdoHcy. With all three compounds, methylated products were not formed (Fig. S9–S13†). In contrast, a clear

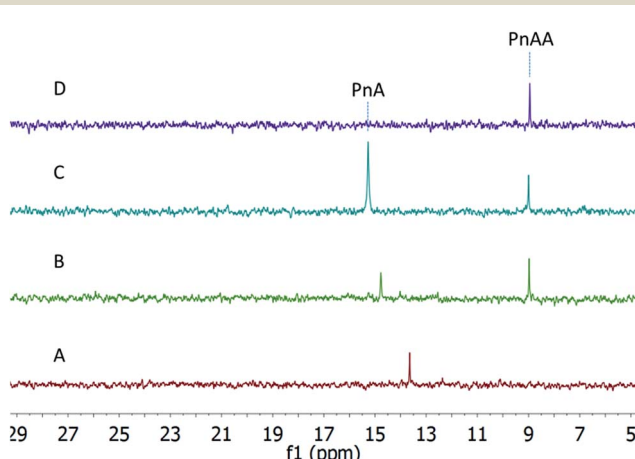
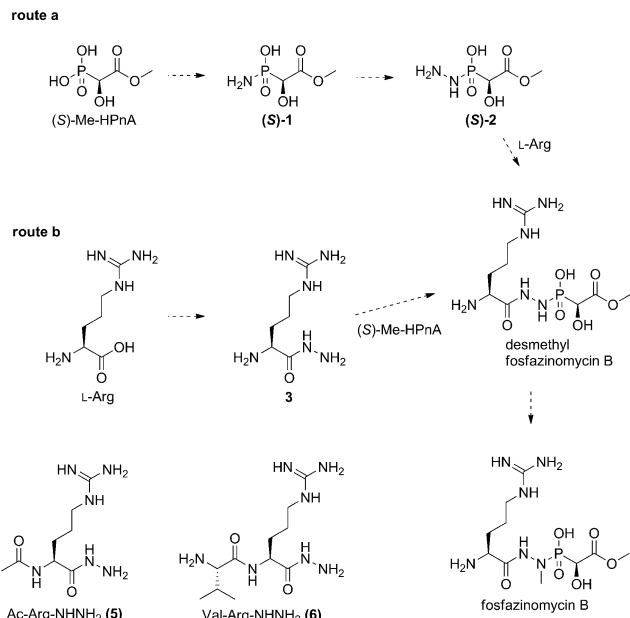


Fig. 4 <sup>31</sup>P NMR spectra of the incubation of His<sub>6</sub>-FzmG with PnAA. (A) NMR spectrum of the reaction mixture containing PnAA, O<sub>2</sub>,  $\alpha$ -KG, Fe(II), L-ascorbate, and His<sub>6</sub>-FzmG. (B) NMR spectrum of the enzymatic reaction mixture spiked with authentic standard of PnAA. (C) NMR spectrum of the reaction mixture spiked with authentic standards of PnAA and PnA. (D) NMR spectrum of the reaction mixture in the absence of His<sub>6</sub>-FzmG. The chemical shifts of phosphonates in <sup>31</sup>P NMR are very sensitive to pH near their  $pK_a$  values, accounting for the changes in chemical shifts between experiments and requiring spiking with standards for assignments.





Scheme 2 Two proposed routes of converting (S)-Me-HPnA to fosB.

new methyl peak was observed in the  $^1\text{H}$  NMR spectrum when Arg-NHNH<sub>2</sub> (3) was incubated with His<sub>6</sub>-FzmH in the presence of SAM. The product was confirmed to be Arg-NHNHMe (4) by spiking with a synthetic authentic standard (Fig. 5B and C), and this assignment was also supported by high resolution Fourier transform MS (Fig. S14 $\dagger$ ). In the absence of His<sub>6</sub>-FzmH, no methylation occurred (Fig. 5A). These results are consistent with a convergent pathway (route b) and not with a linear pathway

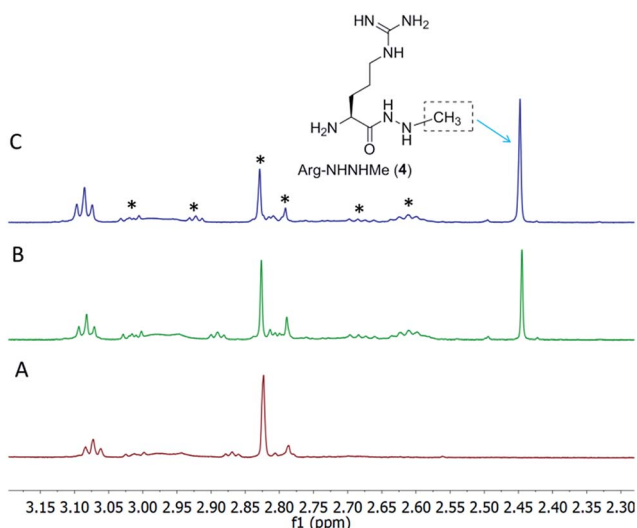


Fig. 5  $^1\text{H}$  NMR spectra of products generated upon incubation of His<sub>6</sub>-FzmH with Arg-NHNH<sub>2</sub> (3). (A) NMR spectrum of the reaction mixture in the absence of His<sub>6</sub>-FzmH. (B) NMR spectrum of the enzymatic reaction mixture containing Arg-NHNH<sub>2</sub>, SAM, AdoHcy nucleosidase, and His<sub>6</sub>-FzmH. (C) NMR spectrum of the reaction mixture spiked with authentic standard of Arg-NHNHMe. The peaks marked with asterisks originate from SAM and SAM-related products.

and provide important insights into the potential identity of substrates for N-N bond formation (e.g. this process does not occur on phosphonate substrates). To further study the substrate specificity of FzmH, Ac-Arg-NHNH<sub>2</sub> (5) and Val-Arg-NHNH<sub>2</sub> (6) (Scheme 2) were synthesized. The enzyme methylated both of these compounds on the terminal nitrogen and the product identity was again confirmed by spiking with synthetic authentic standards (Fig. S15 and S16 $\dagger$ ) and FT-MS (Fig. S17 and S18 $\dagger$ ).

## Discussion

The *O*-methyltransferase His<sub>6</sub>-FzmB methylated both PnA and HPnA with high efficiency *in vitro*, preventing assignment of the physiological substrate. On the other hand, His<sub>6</sub>-FzmG hydroxylated Me-PnA and PnA with very different catalytic efficiencies. The  $K_m$  of Me-PnA was  $0.08 \pm 0.02 \text{ mM}$ , 100-fold lower than that of PnA ( $8 \pm 1 \text{ mM}$ ). Combined with the similar  $k_{\text{cat}}$  values ( $0.27 \pm 0.01 \text{ s}^{-1}$  versus  $0.17 \pm 0.01 \text{ s}^{-1}$ ), these results strongly suggest Me-PnA is the physiological substrate of FzmG. Therefore, methylation of PnA by FzmB likely occurs before hydroxylation. This order of methylation and hydroxylation also matches well with the fact that Me-PnA is one of the observed metabolites produced by fosfazinomycin producing strains.<sup>6</sup>

PnAA is a common intermediate in phosphonate biosynthesis, and it is processed in three different ways in various characterized pathways.<sup>11</sup> PnAA can be converted to 2-aminoethylphosphonate (2-AEP) by a transaminase<sup>12</sup> or reduced to 2-HEP by an alcohol dehydrogenase.<sup>10,13-15</sup> Finally it can also condense with oxaloacetate to give 2-keto-4-hydroxy-5-phosphonopentanoic acid in rhizoctocin biosynthesis.<sup>11,16</sup> To our knowledge, the fosfazinomycin pathway is the first example in which PnAA is transformed to PnA in a phosphonate biosynthetic pathway. We note that the same reaction catalysed by an aldehyde dehydrogenase PhnY was reported in phosphonate catabolic pathways.<sup>11</sup> Our current findings that FzmG was able to generate PnA from PnAA with only 6-fold lower catalytic efficiency compared to its oxidation of Me-PnA ( $k_{\text{cat}}/K_m = 5 \times 10^2 \text{ M}^{-1} \text{ s}^{-1}$  versus  $k_{\text{cat}}/K_m = 3 \times 10^3 \text{ M}^{-1} \text{ s}^{-1}$ ) suggests that FzmG possesses a relaxed substrate specificity. Hence, it is possibly the missing enzyme in our previously proposed fosfazinomycin biosynthetic pathway (Scheme 1). However, we cannot rule out the possibility that a housekeeping aldehyde dehydrogenase outside the gene cluster might oxidize PnAA to PnA. There are other examples of  $\alpha$ -KG dependent non-heme iron dioxygenases catalysing multiple reactions in a single biosynthetic pathway.<sup>17</sup> One such example is the clavaminic acid synthase, which catalyses three separate oxidative steps during clavulanic acid biosynthesis, involving hydroxylation, cyclization and desaturation reactions.<sup>17,18</sup>

Although most secondary metabolites are biosynthesized in a linear fashion, some small molecules, mostly polyketides and non-ribosomal peptides, are generated *via* a convergent manner.<sup>19-21</sup> For example, the chromophore of maduropeptin, an enediyne antitumor compound, was installed from four components using a convergent strategy.<sup>19</sup> In contrast, until this study, all known phosphonates with characterized biosynthetic

pathways were shown to be generated in a linear pathway. Our observation that FzmH can convert Arg-NHNH<sub>2</sub> (3) and related compounds 5 and 6 to their *N*-methylated products, whereas other potential substrates were not accepted, strongly supports methylation of an acylhydrazine during the biosynthesis of fosfazinomycins. In turn, these results indicate that fosfazinomycin B is biosynthesized from two advanced intermediates, Arg-NHNHMe (4) and (S)-Me-HPnA following a convergent manner. The enzymes involved in the formation of 3 and in the condensation reaction remain to be identified among the proteins encoded in the cluster whose functions have not yet been assigned.<sup>6</sup> Such studies can now commence with the knowledge gained about potential substrates in this study.

## Methods

### General methods

For reagents, molecular biology procedures, enzyme purifications, synthetic procedures for the preparation of substrates and standards, and their spectroscopic characterization, see the ESI.†

### FzmB activity assays

The reaction mixture (500 µL) contained 5 mM of the appropriate phosphonic acid, 6 mM *S*-adenosyl methionine (SAM), 0.9 mg mL<sup>-1</sup> AdoHcy nucleosidase, and 74 µM FzmB in 50 mM sodium phosphate (NaPi) buffer, pH 7.7. After 5.5 h incubation at ambient temperature, the proteins were removed by passing the reaction mixture through an Amicon spin column of 10 kDa molecular weight cut-off (MWCO), and 150 µL D<sub>2</sub>O was added into the sample before NMR analysis.

### FzmG activity assays

The reaction mixture (500 µL) contained 5 mM of the appropriate phosphonic acid, 10 mM  $\alpha$ -ketoglutarate, 1 mM L-ascorbic acid, 0.2 mM (NH<sub>4</sub>)<sub>2</sub>Fe(SO<sub>4</sub>)<sub>2</sub>, and 37 µM FzmG in 50 mM NaPi, pH 7.7. Typically the enzyme had been reconstituted in an anaerobic glove box (Coy, Grass Lake, MI) with 1.2 equivalent of Fe(II) for *ca.* 10 min on ice prior to its use. After 5.5 h incubation at ambient temperature, *ca.* 100 µL of Chelex resin was added to the reaction tube. The resin was left to chelate metal ions at room temperature for *ca.* 15 min to reduce line broadening in the NMR spectra. The protein was removed by passing the reaction mixture through an Amicon spin column (10 kDa MWCO), and 150 µL D<sub>2</sub>O was added into the sample before NMR analysis. The assay with PnAA contained 1 mM PnAA, 2 mM  $\alpha$ -ketoglutarate, 0.2 mM L-ascorbic acid, 0.03 mM (NH<sub>4</sub>)<sub>2</sub>Fe(SO<sub>4</sub>)<sub>2</sub>, and 7.4 µM FzmG in 50 mM NaPi, pH 7.7 and was incubated for 7.5 h.

### Kinetic assays with FzmG

A Hansatech O<sub>2</sub> electrode was used to generate the Michaelis-Menten curves by varying the concentration of the appropriate phosphonic acid while keeping  $\alpha$ -KG at a saturating concentration (1 mM) and at a constant FzmG concentration (3.7 µM for Me-PnA, PnAA and 2-HEP assays, and 9.25 µM for PnA

assay). All reactions were initiated by the addition of FzmG, and the initial rate of O<sub>2</sub> consumption was measured in triplicate. Nonlinear regressions were calculated using Igor Pro version 6.1.

### FzmH activity assays

The reaction mixture (500 µL) contained 2.5 mM of the appropriate substrate, 3.5 mM *S*-adenosyl methionine (SAM), 0.9 mg mL<sup>-1</sup> AdoHcy nucleosidase, and 26 µM FzmH in 50 mM NaPi, pH 7.7. After 6.5 h incubation at ambient temperature, the proteins were removed by passing the reaction mixture through an Amicon spin column (10 kDa MWCO), and 150 µL D<sub>2</sub>O was added into the sample before NMR analysis.

## Acknowledgements

We thank Spencer Peck (UIUC) for helpful discussion and Dr Despina Bougioukou (UIUC) for critical reading of this manuscript. This work was supported by the National Institute of Health (GM PO1 GM077596 to W.A.V.). NMR spectra were recorded on a 600 MHz instrument purchased with support from NIH Grant S10 RR028833.

## Notes and references

- 1 W. W. Metcalf and W. A. van der Donk, *Annu. Rev. Biochem.*, 2009, **78**, 65–94.
- 2 S. C. Peck and W. A. van der Donk, *Curr. Opin. Chem. Biol.*, 2013, **17**, 580–588.
- 3 R. M. Cicchillo, H. Zhang, J. A. V. Blodgett, J. T. Whittleck, G. Li, S. K. Nair, W. A. van der Donk and W. W. Metcalf, *Nature*, 2009, **459**, 871–874.
- 4 Y. Kuroda, M. Okuhara, T. Goto, M. Okamoto, H. Terano, M. Kohsaka, H. Aoki and H. Imanaka, *J. Antibiot.*, 1980, **33**, 29–35.
- 5 T. Ogita, S. Gunji, Y. Fukuzawa, A. Terahara, T. Kinoshita, H. Nagaki and T. Beppu, *Tetrahedron Lett.*, 1983, **24**, 2283–2286.
- 6 J. Gao, K. S. Ju, X. Yu, J. E. Velasquez, S. Mukherjee, J. Lee, C. Zhao, B. S. Evans, J. R. Doroghazi, W. W. Metcalf and W. A. van der Donk, *Angew. Chem., Int. Ed.*, 2014, **53**, 1334–1337.
- 7 X. M. Yu, J. R. Doroghazi, S. C. Janga, J. K. Zhang, B. Circello, B. M. Griffin, D. P. Labeda and W. W. Metcalf, *Proc. Natl. Acad. Sci. U. S. A.*, 2013, **110**, 20759–20764.
- 8 K. Schiessl, A. Roller and F. Hammerschmidt, *Org. Biomol. Chem.*, 2013, **11**, 7420–7426.
- 9 B. T. Circello, A. C. Eliot, J. H. Lee, W. A. van der Donk and W. W. Metcalf, *Chem. Biol.*, 2010, **17**, 402–411.
- 10 D. J. Bougioukou, S. Mukherjee and W. A. van der Donk, *Proc. Natl. Acad. Sci. U. S. A.*, 2013, **110**, 10952–10957.
- 11 V. Agarwal, S. C. Peck, J. H. Chen, S. A. Borisova, J. R. Chekan, W. A. van der Donk and S. K. Nair, *Chem. Biol.*, 2014, **21**, 125–135.



12 A. D. Kim, A. S. Baker, D. Dunaway-Mariano, W. W. Metcalf, B. L. Wanner and B. M. Martin, *J. Bacteriol.*, 2002, **184**, 4134–4140.

13 S. C. Peck, S. Y. Kim, B. S. Evans and W. A. van der Donk, *MedChemComm*, 2012, **3**, 967–970.

14 Z. Shao, J. A. Blodgett, B. T. Circello, A. C. Eliot, R. Woodyer, G. Li, W. A. van der Donk, W. W. Metcalf and H. Zhao, *J. Biol. Chem.*, 2008, **283**, 23161–23168.

15 R. D. Woodyer, G. Li, H. Zhao and W. A. van der Donk, *Chem. Commun.*, 2007, 359–361.

16 S. A. Borisova, B. T. Circello, J. K. Zhang, W. A. van der Donk and W. W. Metcalf, *Chem. Biol.*, 2010, **17**, 28–37.

17 R. P. Hausinger, *Crit. Rev. Biochem. Mol. Biol.*, 2004, **39**, 21–68.

18 M. D. Lloyd, K. D. Merritt, V. Lee, T. J. Sewell, B. Wha-Son, J. E. Baldwin, C. J. Schofield, S. W. Elson, K. H. Baggaley and N. H. Nicholson, *Tetrahedron*, 1999, **55**, 10201–10220.

19 S. G. Van Lanen, T. J. Oh, W. Liu, E. Wendt-Pienkowski and B. Shen, *J. Am. Chem. Soc.*, 2007, **129**, 13082–13094.

20 H. A. Cooke, E. L. Guenther, Y. G. Luo, B. Shen and S. D. Bruner, *Biochemistry*, 2009, **48**, 9590–9598.

21 T. D. Nusca, Y. Kim, N. Maltseva, J. Y. Lee, W. Eschenfeldt, L. Stols, M. M. Schofield, J. B. Scaglione, S. D. Dixon, D. Oves-Costales, G. L. Challis, P. C. Hanna, B. F. Pfleger, A. Joachimiak and D. H. Sherman, *J. Biol. Chem.*, 2012, **287**, 16058–16072.

